



HAL
open science

Thermodynamic study of the sodium chromite NaCrO₂

Sylvie Chatain, Nicolas David, David Bonina, Jean-Louis Fleche, Christophe Bonnet, Jean-Louis Courouau, Marion Rouhard

► **To cite this version:**

Sylvie Chatain, Nicolas David, David Bonina, Jean-Louis Fleche, Christophe Bonnet, et al.. Thermodynamic study of the sodium chromite NaCrO₂. Journal of Alloys and Compounds, 2021, 882, pp.160784. 10.1016/j.jallcom.2021.160784 . cea-03552286

HAL Id: cea-03552286

<https://cea.hal.science/cea-03552286>

Submitted on 2 Aug 2023

HAL is a multi-disciplinary open access archive for the deposit and dissemination of scientific research documents, whether they are published or not. The documents may come from teaching and research institutions in France or abroad, or from public or private research centers.

L'archive ouverte pluridisciplinaire **HAL**, est destinée au dépôt et à la diffusion de documents scientifiques de niveau recherche, publiés ou non, émanant des établissements d'enseignement et de recherche français ou étrangers, des laboratoires publics ou privés.



Distributed under a Creative Commons Attribution - NonCommercial 4.0 International License

Thermodynamic study of the sodium chromite NaCrO₂

Sylvie Chatain^{1*}, Nicolas David², David Bonina², Jean-Louis Flèche¹, Christophe Bonnet¹, Jean-Louis Courouau¹ and Marion Rouhard¹

¹ Université Paris-Saclay, CEA, Service de la Corrosion et du Comportement des Matériaux dans leur Environnement, 91191, Gif-sur-Yvette, France

² Université de Lorraine, CNRS, Institut Jean Lamour, 54011, Nancy, France

Corresponding author: E-mail address: sylvie.chatain@cea.fr, Full postal address: CEA Saclay, DPC/SCCME/LM2T PC n°50, 91191, Gif-sur-Yvette, France

Abstract

A thermodynamic study was undertaken on two kinds of NaCrO₂(s) powder, a commercial and an experimental one synthesized. Heat capacity measurements were carried out in the temperature range of 25 °C to 600 °C using a differential scanning calorimeter. Gibbs energy of formation versus temperature was deduced using these experimental data, the enthalpy of formation from literature and the entropy at room temperature deduced from *ab initio* calculations combining with a quasi-harmonic statistical model. The equation obtained is given by:

$$\Delta_f G^\circ(T) (\text{NaCrO}_2) (\text{kJ/mol O}_2) = -876.094 + 0.191 \times T (\pm 2\%).$$

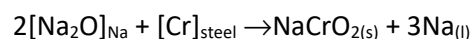
The temperature of phase transition measured by differential thermal analysis at (819±4) °C is slightly higher than the temperature in the literature attributed to the decomposition of NaCrO₂ into Cr₂O₃ and Na₂O. However, the X-ray diffraction patterns showed only NaCrO₂ phase which didn't confirm the decomposition reaction.

Key words: Sodium chromite, Differential Scanning Calorimetry, Differential Thermal Analysis, Ab initio calculations, Quasi-harmonic model

1- Introduction

In nominal conditions, fast sodium reactor materials are subject to corrosion. Numerous experimental studies have shown that the behaviour of materials in liquid sodium at high temperature (≥500°C) is influenced by their interaction with the dissolved oxygen. The sodium chromite, NaCrO₂, is one of the most important corrosion product observed on stainless steel surface [1] in contact with liquid sodium. Its formation depends on the threshold oxygen level in sodium but there is considerable discrepancy between theoretically calculated values and experimental data.

The equation for the formation of NaCrO₂ in a sodium/steel system is written as:



where [Cr]_{steel} represents the chromium contained in the steel. The standard Gibbs energy of this reaction is expressed as [2]:

$$\Delta_r G^0 = \Delta_f G^0(\text{NaCrO}_2) - 2\Delta_f G^0(\text{Na}_2\text{O}) = 2RT \ln \left(\frac{C_0}{C_0^{\text{sat}}} \right) + RT \ln a_{\text{Cr}}$$

with C₀ concentration of oxygen in sodium, C₀^{sat} concentration of oxygen at saturation and a_{Cr} chromium activity in steel.

The input data required for the calculation of the threshold oxygen level (C_0) are the Gibbs energy of formation of NaCrO_2 , and Na_2O , the solubility of oxygen in liquid sodium (C_0^{sat}) and the activity of chromium in the steel at the relevant temperature. A sensitivity analysis showed that among these data, the dispersion of the Gibbs energy of formation data has a main effect of the threshold oxygen value (from 0.078 ppm to 9.934 at 800 K). So, there is a need of accurate Gibbs energy of formation of NaCrO_2 . Different reasons mentioned by some authors and reminded in Part 2 can explain this discrepancy such as i) the possibility of electronic conduction in yttria doped thoria (YDT) in electromotive force (e.m.f) measurements, ii) the use of different thermodynamic data resulted differing results (ex $\Delta_f \tau G^\circ(\text{Na}_2\text{O})$), iii) the uncertainty of the stoichiometry and thermodynamic data of ternary compounds (Na_4CrO_4 for example) involving in equilibria and iv) the reactivity of the liquid sodium with the crucible material. To avoid these problems, in this work we have provided thermodynamic data of NaCrO_2 firstly experimentally by using only NaCrO_2 compound and secondly theoretically with Density Functional Theory calculations.

2- Literature review of thermodynamic properties

There is considerable discrepancy in the literature on the Gibbs energy of formation of the sodium chromite versus temperature (Figure 1). Two experimental techniques are used: the electromotive force measurements (e.m.f) [3-10] and the measurement of the equilibrium pressure by Knudsen cell mass spectrometry (KC) [8] [11-12].

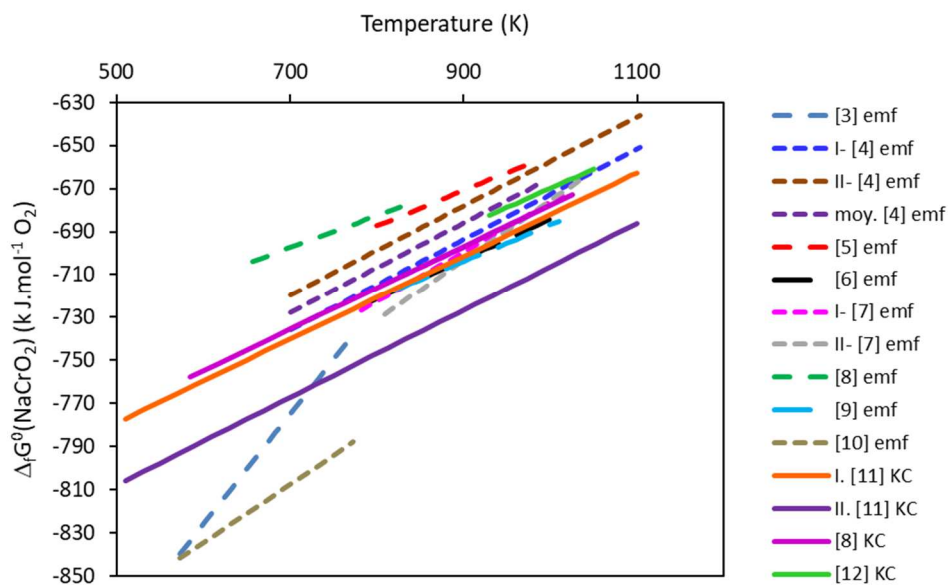


Figure 1 $\Delta_f G_T^0(\text{NaCrO}_2)$ values from literature (raw values); electromotive force measurements (e.m.f) and Knudsen cell measurements (KC)

The Gibbs energy of formation can also be calculated from the heat capacity measurement knowing the enthalpy of formation and the entropy of the compound at 25 °C.

The enthalpy of formation has been deduced from calorimetric measurements made both of the heat of combination of the Na_2O and Cr_2O_3 oxides and the heat of solution in hydrochloric acid [13]. They lead to a similar value of $\Delta_f H^\circ = -101.4 \pm 1.0 \text{ kJ.mol}^{-1}$ which gives the standard enthalpy of formation of $\Delta_f H_{298 \text{ K}}^\circ = -874.2 \pm 7.3 \text{ kJ.mol}^{-1}$ (accuracy deduced from the uncertainty of the enthalpy of reaction and uncertainties found for the enthalpy of formation of Na_2O and Cr_2O_3 [14]). The enthalpy of formation of NaCrO_2 from Na_2O and Cr_2O_3 was studied by differential scanning

calorimetry (DSC) in the temperature range 240 °C to 490 °C by Van Vuuren [15]. He found $\Delta_f H^\circ = -142.0 \pm 3.8 \text{ kJ.mol}^{-1}$ which is higher than [13] one. It was also calculated mixing generalized gradient approximation (GGA) and GGA+U. The value $\Delta_f H^\circ_{298 \text{ K}} = -883.1 \text{ kJ.mol}^{-1}$ [16] is in good agreement with the experimental result of Gross *et al.* [13].

The heat capacity was measured by DSC from 77 °C to 327 °C by Sreedharan *et al.* [6]. They gave: $C_p \text{ (J.K}^{-1}.\text{mol}^{-1}) = 27.15 + 0.1247 \times T \text{ (K)}$ which is completely different of the equation given by Iyer *et al.* [17] $C_p \text{ (J.K}^{-1}.\text{mol}^{-1}) = -75.364 + 0.02512 \times T \text{ (K)}$ and deduced from the first differential of the enthalpy increment measurements with temperature carried out in the 50 °C to 566 °C temperature range using a high temperature Calvet micro calorimeter.

Finally, concerning the thermal stability of $\text{NaCrO}_2(\text{s})$, on one hand following Barker *et al.* [18] $\text{NaCrO}_2(\text{s})$ decomposes into $\text{Na}_2\text{O}(\text{s})$ and $\text{Cr}_2\text{O}_3(\text{s})$ at 795 °C whereas on the other hand following Sampath [19], the compound is stable until 1200 °C under argon.

So in order to resolve the discrepancy and improve the knowledge of the thermodynamic properties of the sodium chromite, after a critical analysis of the Gibbs energy of formation of NaCrO_2 , the heat capacity measurements was performed by DSC and the Gibbs energy of formation was then deduced. Thermodynamic functions were calculated by combining ab initio calculations and a quasi-harmonic statistical model. Finally, the study was completed with the decomposition temperature determination by differential thermal analysis (DTA).

3- Critical analysis of the Gibbs energy of formation measurements

The studies performed to determine the standard Gibbs energy of formation of sodium chromite are collected in Table 1: in the upper part, we find the e.m.f studies and in the lower part the Knudsen cell mass spectrometry results. We have compared the results according different criteria: the experimental method (e.m.f or mass spectrometry) and a given equilibrium studied with both methods.

3.1- e.m.f measurements

At first, we have excluded the data of Janson *et al.* [3] and Blokhin *et al.* [10] which are very away from the other results. Three equilibria were studied: $\text{Na(l)} + \text{Cr(s)} + \text{NaCrO}_2(\text{s})$ [5] [8], $\text{NaCrO}_2(\text{s}) + \text{Cr(s)} + \text{Cr}_2\text{O}_3(\text{s})$ [4] [7] and $\text{NaCrO}_2(\text{s}) + \text{Cr}_2\text{O}_3(\text{s}) + \text{Na}_2\text{CrO}_4(\text{s})$ [6] [9]. If we compare the results obtained for each equilibria, we note that:

- For the $\text{NaCrO}_2(\text{s}) + \text{Cr(s)} + \text{Cr}_2\text{O}_3(\text{s})$ equilibrium, there is a good agreement between Bhat *et al.* [7] and Shaiu *et al.* [4] for the temperature higher than 727 °C (1000 K)
- For the $\text{Na(l)} + \text{Cr(s)} + \text{NaCrO}_2(\text{s})$ equilibrium, the agreement is good between the studies (1% discrepancy at 327 °C (600 K)) but it seems that there was a problem of electronic conductivity in yttria doped thoria [8]
- There is a very good agreement for the $\text{NaCrO}_2(\text{s}) + \text{Cr}_2\text{O}_3(\text{s}) + \text{Na}_2\text{CrO}_4(\text{s})$ equilibrium [6] [9].

Furthermore, the results obtained with liquid sodium can not be taken into account due to the high reactivity of liquid sodium with crucible material. We noted that these data are the most in disagreement with other values. The sample can thus be polluted and the measurements corrupted. We have retained the data coming from $\text{NaCrO}_2(\text{s}) + \text{Cr(s)} + \text{Cr}_2\text{O}_3(\text{s})$ equilibrium because the uncertainty on the oxide stoichiometry was lower and the kinetic effect was reduced with the presence of pure chromium.

3.2- Equilibrium pressure measurement by Knudsen cell mass spectrometry

Two equilibria were investigated: $\text{NaCrO}_2(\text{s})+\text{Cr}(\text{s})+\text{Cr}_2\text{O}_3(\text{s})$ [8], [12], [11] and $\text{NaCrO}_2+\text{Na}_2\text{O}+\text{Na}_4\text{CrO}_4$ [11]. The agreement is correct between the authors within uncertainties that are important for Knight's results. The values obtained by Knight for the second equilibrium with $\text{NaCrO}_2+\text{Na}_2\text{O}+\text{Na}_4\text{CrO}_4$ were omitted because the uncertainty is important (kinetics problema and/or oxides stoichiometry).

3.3- Comparison of the two experimental methods for a same equilibria

$\text{NaCrO}_2(\text{s})+\text{Cr}(\text{s})+\text{Cr}_2\text{O}_3(\text{s})$ equilibrium was studied both by e.m.f and pressure measurement by Knudsen cell mass spectrometry, [8] [12] [11] [4] [7]. We can conclude that the results remained scattered whatever the experimental method and it is difficult to select an equation.

Experimental method	T(K)	Equilibrium studied	$\Delta_{f,T}G^\circ(\text{NaCrO}_2)$ (kJ/mol O ₂)	Ref.
e.m.f. Air, Pt/YDT*/Na(l), O (Na) *Yttria doped Thoria	573-773	Na(l)-Cr(s)-NaCrO ₂ (s)	-1132+0.510xT (fit of experimental points)	[3]
e.m.f I. Ca,CaF ₂ /CaF ₂ /NaCrO ₂ ,Cr,Cr ₂ O ₃ ,NaF II. NaCrO ₂ ,Cr,Cr ₂ O ₃ ,NaF/CaF ₂ /NiF ₂ ,Ni	700-1100	NaCrO ₂ -Cr-Cr ₂ O ₃	I. -883.368+ 0.2108xT II. -864.707+0.2074xT Average . -874+0.209xT (±8.4 kJ/mol)	[4]
e.m.f In, In ₂ O ₃ /YDT/Na,Na ₂ O	800-980	Na(l)-Cr(s)-NaCrO ₂ (s)	-819.409+0.16508xT	[5]
e.m.f Pt, NaCrO ₂ , Cr ₂ O ₃ , Na ₂ CrO ₄ / 15 YSZ* / O ₂ (air), Pt (*15 w% zirconia stabilised Yttria)	784-1012	NaCrO ₂ -Cr ₂ O ₃ -Na ₂ CrO ₄	-869.98+0.18575xT (±1.86 kJ/mol)	[6]
e.m.f In, In ₂ O ₃ /YDT/Na,Cr,NaCrO ₂	657-825	Na(l)-Cr(s)-NaCrO ₂ (s)	-800.847+0.14785xT (±1.35 kJ/mol)	[8]
e.m.f I. Pt,NaCrO ₂ ,Cr,Cr ₂ O ₃ ,NaF/CaF ₂ /Co,CoF ₂ ,Pt II. Pt,NaCrO ₂ ,Cr,Cr ₂ O ₃ ,NaF/CaF ₂ /Ni,NiF ₂ ,Pt	782-1014 809-1040	NaCrO ₂ -Cr-Cr ₂ O ₃	I. -908+0.2317xT (±1.6 kJ/mol) II. -953.5+0.278xT (±3.3 kJ/mol)	[7]
e.m.f Pt/NaCrO ₂ +Na ₂ CrO ₄ +Cr ₂ O ₃ /(1-x)ZrO ₂ +xCaO/air/Pt	820-1006	NaCrO ₂ -Cr ₂ O ₃ -Na ₂ CrO ₄	-856.1+0.1693xT (±2.5 kJ/mol)	[9]
e.m.f Me/In-In ₂ O ₃ /electrolyte/Na-Cr-NaCrO ₂ /Me	573-773	Na(l)-Cr-NaCrO ₂	-995.79+0.269xT	[10]
Knudsen cell mass spectrometry (Mo crucible)	825-1025	NaCrO ₂ -Cr ₂ O ₃ -Cr	-870.773+0.193171xT	[8]
Knudsen –effusion mass-loss(stainless steel crucible)	930-1044	NaCrO ₂ (s)-Cr ₂ O ₃ (s)-Cr(s)	-847.0+0.1772xT (±3.7 kJ/mol)	[12]
Knudsen cell mass spectrometry (Thoria liners in Ni or stainless steel crucible)	510-1000 660-890	I. NaCrO ₂ (s)-Cr ₂ O ₃ (s)-Cr(s) II. NaCrO ₂ (s)-Na ₄ CrO ₄ (s)-Na ₂ O(s)	I. -(876±18)+(0.194±0.009)xT II. -(909.4±27)+(0.203±0.029)xT	[11]

Table 1 Experimental Gibbs energy of formation of NaCrO₂ reported in the literature

4- Materials and methods

4.1- NaCrO₂

Two sets of sodium chromite were studied: one commercial from Neyco (purity 99 %) and the other synthesized at CEA (Non aqueous corrosion study laboratory). The commercial NaCrO₂ was irregular chips with 1 to 10 mm size (Figure 2a).

Synthesized NaCrO₂ was prepared according the method described by [20] [21] [22]. Equimolar quantities (0.0322 mol) of carbonate sodium, Na₂CO₃ (anhydrous, AnalaR Normapur, purity 99.9 %), and chromine Cr₂O₃ (Alfa Aesar, purity 99%) (Figure 2b) were heated with a 7.8 °C.min⁻¹ rate in a slight neutral argon flow (~7L/h) between 850 °C and 900 °C for 5h. The solid state reaction led to the formation of sodium chromite following:



The granulometry of the powder must be as fine as possible to improve the contact between the reactives and thus the reactivity. The oxygen partial pressure was measured with a Zirox probe at the exit of the furnace. The weight loss was controlled to follow the progress of the chemical reaction. The heat treatment was repeated until the complete reaction of NaCO₃ and Cr₂O₃ and controlled by X ray diffraction. The green powder obtained (Figure 2c) was kept in a glove box under dry nitrogen.



a)

b)

c)

Figure 2. . a) commercial Neyco NaCrO₂; b) Na₂CO₃ and Cr₂O₃ powder mixture ; c). NaCrO₂ synthesized

4.1.1 X ray diffraction (XRD)

XRD measurements have been carried out using the Bruker D8 discover device diffractometer with a Cu (K α 1) radiation ($\lambda = 1.5406\text{\AA}$). The grinded powder was analysed in an airtight dome, under argon atmosphere. We showed that the peaks related to the reactives Na₂CO₃ and Cr₂O₃ disappeared particularly the most intense at 30.3 °, 55° and 63.6° for the chromine and 30.3° and 38.2° for the sodium carbonate (Figure 3). It confirmed that the reaction was complete within the method error (0.5% in volume). The diffractogram obtained for the experimental product is in agreement with the NaCrO₂ identification databank.

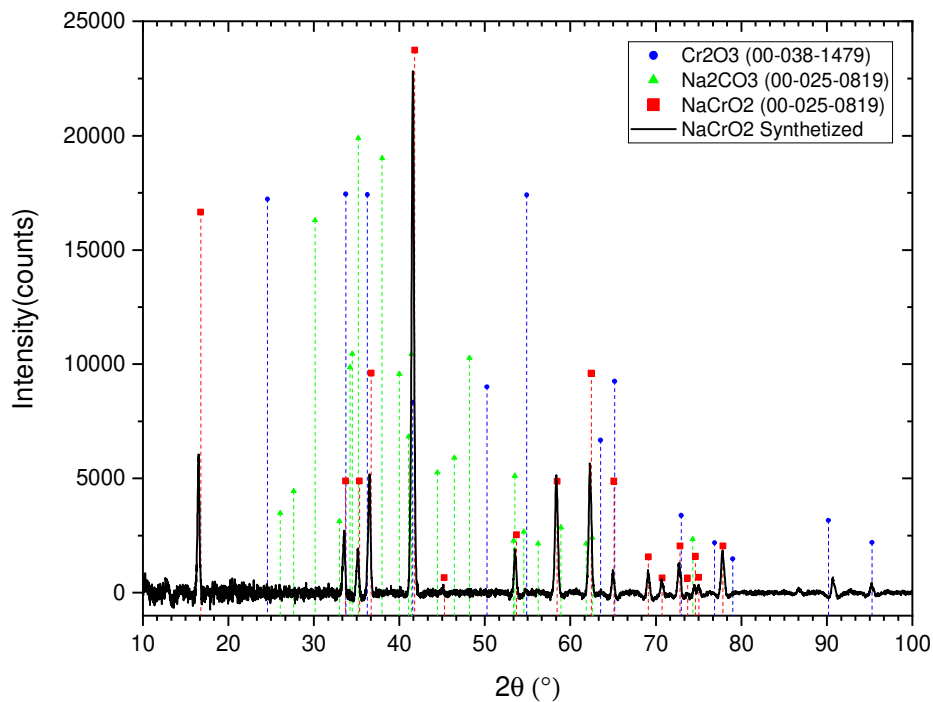
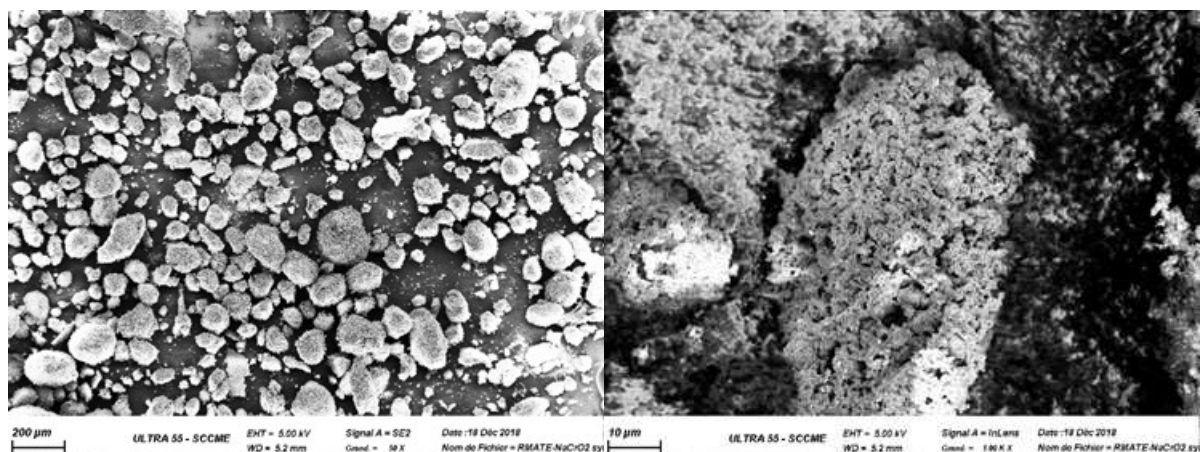


Figure 3. Indexation of XRD diffractogram of NaCrO_2 synthesized in this work from Na_2CO_3 and Cr_2O_3 (International Center for Diffraction Data); NaCrO_2 is NaFeO_2 prototype, with hexagonal symmetry, space group $R\bar{3}m$, $Z=3$, cell parameters $a=2.9747\pm 0.0001 \text{ \AA}$, $c=15.9538\pm 0.0003 \text{ \AA}$ [23]

4.1.2- Morphology of the synthesized compound

The morphology of the synthesized compound was analysed by Scanning Electron Microscopy (SEM). SEM pictures are obtained with a Zeiss Gemini ultra 55. The NaCrO_2 powder had grains size between 40 and 200 μm (Figure 4) with a mean value of about 100 μm . The morphology was rounded but the grains were very porous which was very similar with the morphology obtained by Ding *et al.* [22] and Chen *et al.* [24].



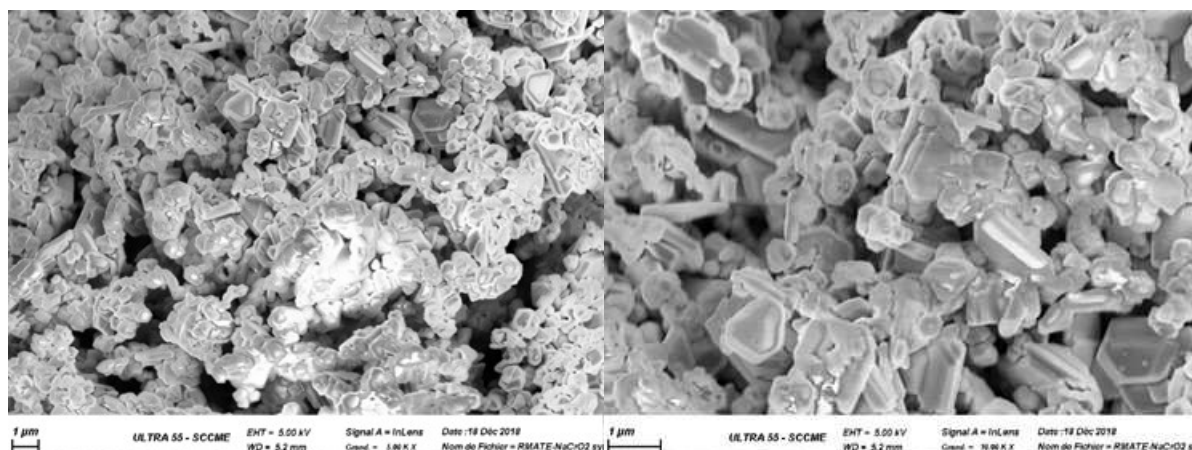


Figure 4. SEM pictures of the NaCrO_2 grains at different magnification (x50, x1000, x5000, x10000, from up to down and left to right)

4.1.3- Impurity dosage

Glow Discharge- Mass Spectrometry (GD-MS) can be used to analyze the chemical composition of a powder after grinding and amalgamating in an ultra-pure silver pellet (Ag Alfa Aesar 99.999 %). This new technique is more accurate and avoid the potential pollution of the sample due to the different steps of the high temperature alkaline dissolution. The impurity contents in both experimental and commercial sodium chromite are shown Table 2.

Element	Impurity content	Element	Impurity content
B	7	Co	0.75
Mg	25	Ni	5.5
Al	50	Cu	25
Si	70	Zn	0.8
P	12	Sr	10
S	45	Zr	<5
Ca	25	Mo	2.1
Ti	0.85	Sn	0.5
V	<3	Ba	3.1
Mn	<3	Ta	2.0
Fe	250	Pb	0.2

a)

Element	Impurity content	Element	Impurity content
B	5	Co	1.0
Mg	20	Ni	3.0
Al	130	Cu	10
Si	250	Zn	0.4
P	7	Sr	0.1
S	20	Zr	<5
Ca	5	Mo	1.1
Ti	1.2	Sn	0.1
V	1.0	Ba	2.1
Mn	<3	Ta	0.2
Fe	400	Pb	1.0

b)

Table 2. GDMS analysis results in $\mu\text{g}\cdot\text{g}^{-1}$. Elements with a content $<0.1 \mu\text{g}\cdot\text{g}^{-1}$ are not mentioned. a) experimental NaCrO_2 ; b) commercial NaCrO_2

4.2- Differential Scanning calorimetry

The purity of the compounds was checked upon receipt by XRD. The narrow peaks indicated a monophasic compounds. Before the heat capacity measurements, the thermal stability of both powders was checked up to 600°C under argon by recording diffractograms with temperature between 250°C and 600°C . No supplementary peak was detected which confirmed that NaCrO_2 is stable until 600°C in agreement with Barker *et al.* [18] and Sampath *et al.* [19] results.

The heat capacity measurements were performed with a SETARAM DSC-111 apparatus using alumina crucible. The calibration of the apparatus is done in two parts. At first, the calibration in temperature is obtained from a fit of the melting temperature of pure metals used as standard. These pure metals are sealed under vacuum in very little quartz tubes, heated and cooled from room temperature to 800°C . Pure metals selected are In, Sn, Pb, Zn and Al, covering thus the whole range of temperature of the apparatus. Secondly, the calibration in energy is obtained by the integration of the DSC signal corresponding to the melting of the same pure elements.

Several primary purges following by an argon flow were carried out to reduce the presence of adsorbed gas. The powder was kept at 30°C during 30 minutes and then heated by successive isothermal steps every 20°C up to about 600°C . Each isothermal step time was one hour and the heating rate between two steps $10^\circ\text{C}\cdot\text{min}^{-1}$. After the higher temperature step, the powder was cooled with a $10^\circ\text{C}\cdot\text{min}^{-1}$ down to room temperature. This thermal cycle under argon flow was repeated a second time before opening the apparatus. Each powder has undergone the double thermal cycle twice. The gain or loss of mass of the sample was controlled by weighting. The same temperature program was employed for the blank run using empty crucibles for both sample and reference cells.

4.3- Differential Thermal Analysis (DTA)

DTA measurements were performed using SETARAM apparatus (TG-DTA Setsys). During the analysis, a constant flow of $1 \text{ L}\cdot\text{h}^{-1}$ of pure argon gas (Air Products 99.9997 % purity) was maintained. The crucible closed with a lid was made of platinum. A second lid of silica covered the platinum lid to trap the alkaline vapour. To determine the decomposition temperature at the thermodynamic equilibrium (rate=0), the temperature was measured at three different rates on heating 5°C , 7°C and 10°C per minute. It was taken at the onset temperature of the heat flow peak reduced to the blank line recorded in the same conditions than the experience. The temperature was measured by a platinum rhodium PtRh 6%/30% thermocouple. The calibration of the temperature was performed by using pure metals aluminium, gold and palladium.

5- Ab initio calculations coupled with a quasi-harmonic model

This experimental work was completed with a computational study based on *ab initio* calculations and a quasi-harmonic statistical model. The method used to derive the temperature dependency of the thermodynamic properties, is briefly described hereafter. A more exhaustive description can be found in [25].

5.1- Method to calculate the thermodynamic functions

This method requires only information on the crystal symmetry and space group, lattice parameters, and atomic position coordinates as starting point. The following three approximations are used to derive the free energy of a crystal containing N cells with n atoms per cell:

(i) The adiabatic approximation to calculate the total energy of the crystal $E(V)$ versus (hydro)static pressure, and correspondingly versus the volume. $E(V)$ is the total energy of the static lattice in which each atom occupies its mean position.

(ii) The harmonic approximation to calculate the $3n$ vibration frequencies $\nu_j(\vec{q})$ ($j=1,3n$) for N values of wave vector \vec{q} in the first Brillouin zone. These $3n$ frequencies dispersion branches are divided into three acoustic branches and $(3n-3)$ optical branches. In order to make *ab initio* computations tractable, these vibration frequencies are calculated at the Γ point only ($\vec{q} = 0$). For $\vec{q} \neq 0$ we use the Debye model to determine the acoustic vibration frequencies and the Einstein model for the optical vibration frequencies. From $E(V)$ and the frequencies $\nu_j(\vec{q}=0)$ ($j=1,3n$) it is possible to construct the partition function of the crystal and deduce its free energy at temperature T by the statistical thermodynamic laws:

$$F(T, V) = E(V) + Nk_B T \left[\frac{9}{8} x_D + 3 \ln(1 - e^{-x_D}) - D(x_D) + \sum_{j=4}^{3n} \left(\frac{x_j}{2} + \ln(1 - e^{-x_j}) \right) \right] \quad (1)$$

where $x_j = h \nu_j(0) / k_B T$. $D(x_D)$ is the Debye function with $x_D = \Theta_D / T$ where Θ_D is the Debye temperature. k_B and h are respectively the Boltzmann and Planck constants. For an ideal isotropic crystal [25] Θ_D is given by:

$$\Theta_D = \frac{h}{k_B} \left(\frac{9}{4\pi V} \right)^{1/3} \left(3 \frac{B}{\rho} \right)^{1/2} \left(\frac{1-\sigma^0}{1+\sigma^0} \right)^{1/2} \left(1 + 2 \left(\frac{2-2\sigma^0}{1-2\sigma^0} \right)^{3/2} \right)^{-\frac{1}{3}} \quad (2)$$

B is the bulk modulus, ρ the density and σ^0 the Poisson ratio (close to 0.33).

-(iii) to account for the thermal expansion while maintaining the simplicity of the harmonic model, quasi-harmonic approximation is used assuming that the vibration frequencies change with the volume of the unit cell:

$$pV = -V \frac{dE(V)}{dV} + Nk_B T \left[\gamma_{\text{acoustic}} \left(\frac{9}{8} x_D + 3D(x_D) \right) + \gamma_{\text{optic}} \sum_{j=4}^{3n} \left(\frac{x_j}{2} + \frac{x_j}{e^{x_j} - 1} \right) \right] \quad (3)$$

where γ_{acoustic} and γ_{optic} are the Gruneisen coefficients. For an ideal isotropic crystal these Gruneisen coefficients are given by [25]:

$$\gamma_{\text{acoustic}} = -\frac{2}{3} - \frac{1}{2} V \frac{d}{dV} \ln \left(\frac{d^2 E(V)}{dV^2} \right) \quad (4)$$

$$\gamma_{\text{optic}} = \frac{1}{2} V \frac{d}{dV} \ln \left(\frac{d^2 E(V)}{dV^{2/3}} \right) \quad (5)$$

The volume V is calculated iteratively for a given pressure p and temperature T , knowing $E(V)$ and the vibration frequencies at Γ point, as well as the Poisson ratio σ^0 for the crystal to zero static pressure.

All the thermodynamic functions are calculated from $F(T, V)$ and pV :

- the entropy $S = -(dF/dT)_V$,
- the internal energy $U = F + TS$,
- the heat capacity at constant volume $C_V = (dU/dT)_V$,
- the bulk modulus $B = -V(dp/dV)_T$,
- the thermal expansion $\alpha_p = (dp/dT)_V / B$,

From these functions we can calculate the heat capacity at constant pressure :

$$C_p = C_V + TVB\alpha_p^2 \quad C_p = C_{V \text{ acoustic}} + C_{V \text{ optic}} + T \left(\gamma_{\text{acoustic}} C_{V \text{ acoustic}} + \gamma_{\text{optic}} C_{V \text{ optic}} \right)^2 / (BV)$$

where:

$$BV = V^2 \frac{d^2 E(V)}{dV^2} + \left(\gamma_{\text{acoustic}}^2 + \gamma_{\text{acoustic}} - V \frac{d\gamma_{\text{acoustic}}}{dV} \right) U_{\text{acoustic}} - T \gamma_{\text{acoustic}}^2 C_{v \text{ acoustic}} + \left(\gamma_{\text{optic}}^2 + \gamma_{\text{optic}} - V \frac{d\gamma_{\text{optic}}}{dV} \right) U_{\text{optic}} - T \gamma_{\text{optic}}^2 C_{v \text{ optic}}$$

with:

$$C_{v \text{ acoustic}} = Nk_B \left(12D(x_D) - 9 \frac{x_D}{e^{x_D} - 1} \right)$$

$$C_{v \text{ optic}} = Nk_B \sum_{i=4}^{3n} x_i^2 \frac{e^{x_i}}{e^{x_i} - 1}$$

$$U_{v \text{ acoustic}} = Nk_B T \left(\frac{9}{8} x_D + 3D(x_D) \right)$$

$$U_{v \text{ optic}} = Nk_B T \sum_{i=4}^{3n} \frac{x_i}{2} + \frac{x_i}{e^{x_i} - 1}$$

5.2- Results

Our calculations ($E(V)$ and the vibration frequencies at Γ point) were performed using the CASTEP code [26], which solves the electronic Schrödinger equation for a compound with a periodic lattice within the electronic Density Functional (DFT) Theory using a plane-wave pseudo-potential method. The tightly bound core electrons are represented by non-local ultrasoft pseudo-potentials as proposed by Vanderbilt [27]. The exchange/correlation energies are calculated using the Perdew *et al.* (PBE) form of the Generalized Gradient Approximation (GGA) [28]. The first Brillouin zone is approximated with finite sampling of k-points using the Monkhorst-Pack scheme [29]. Furthermore, when the electron spins of the ions are unpaired the calculations are carried out using polarized spins. NaCrO₂ is known to be an antiferromagnetic compound with trivalent chromium. The search for an antiferromagnetic structure having the stoichiometry of NaCrO₂ is not easy. Assuming that the energy with the antiferromagnetic configuration is not very different with the ferromagnetic configuration, we calculated the energy $E(V)$ with this last configuration. The results of these calculations are given in Table 3, Table 4 and Figure 5.

	Z	a(Å)	b(Å)	c(Å)	α	β	γ	V_0 (Å ³)	B_0 (GPa)	B'_0
Exp.	3	2.968	2.968	15.94	90	90	120	120.645		
Calc.		<i>3.028</i>	<i>3.028</i>	<i>15.984</i>	<i>90</i>	<i>90</i>	<i>120</i>	<i>127.022</i>	<i>121.14</i>	<i>3.65</i>

Table 3. NaCrO₂ parameters and results of the *ab initio* calculations using the CASTEP Code [26]. DFT lattice parameters, equilibrium volume of unit cell, bulk modulus and its derivative with respect to pressure at zero pressure in italics, are compared to the reference experimental data [18].

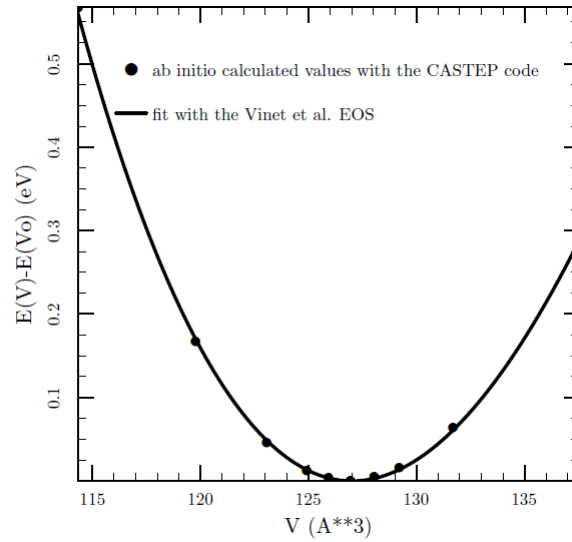


Figure 5. Solid line is energy-volume relationship based on a fit with the Vinet *et al.* [30] integrated equation of state for NaCrO₂. The circles are the energies calculated values with the CASTEP code in DFT/GGA.

Vibrational frequency (degeneracy)
69.135847 cm ⁻¹ (4)
126.073050 cm ⁻¹ (2)
153.784178 cm ⁻¹ (4)
170.803531 cm ⁻¹ (2)
284.958325 cm ⁻¹ (1)
305.271195 cm ⁻¹ (2)
408.208746 cm ⁻¹ (4)
410.547233 cm ⁻¹ (2)
415.498866 cm ⁻¹ (2)
419.262014 cm ⁻¹ (4)
497.073448 cm ⁻¹ (1)
526.283746 cm ⁻¹ (1)
537.228558 cm ⁻¹ (2)
580.187810 cm ⁻¹ (2)

Table 4. The Γ point harmonic vibrational frequencies and degeneracy computed with the CASTEP code by diagonalizing the mass-weighted second-derivative Hessian matrix.

To fit the theoretical heat capacity at constant pressure it is convenient to use the following regression law:

$$C_p (J.mol^{-1}.K^{-1}) = 97.42 + 1.46 \times 10^{-6} T^2 + 0.00792 T - 1532260 T^{-2}$$

Theoretical entropy of NaCrO₂ is obtained with

$$S = Nk_B \left(4D(x_D) - 3 \ln(1 - e^{-x_D}) + \sum_{i=1}^{3n} \frac{x_i}{4e^{x_i} - 1} - \ln(1 - e^{-x_D}) \right)$$

The corresponding theoretical standard heat capacity and entropy functions at 298.15 K are 82.9 J.K⁻¹.mol⁻¹ and 94.5 J.K⁻¹.mol⁻¹ respectively.

6- Results and discussion

6.1- Heat capacity measurements

Both sodium chromite were studied in the temperature range of 25 °C - 600 °C: the commercial and the experimental. From the obtained curves, heat capacities, $C_{p,m}(T)$, at a given temperature T can be calculated by integrating the variation of the calorimetric signal reduced of the blank signal between two successive isothermal steps. The experimental results of the heat capacity for both commercial and experimental sodium chromite are presented in Figure 6. The heat capacity values are similar and increase slightly with temperature. The points dispersion for each temperature is a little more important for the experimental powder than for the commercial one (3% versus 2% in average) but we have no explanation for this observation.

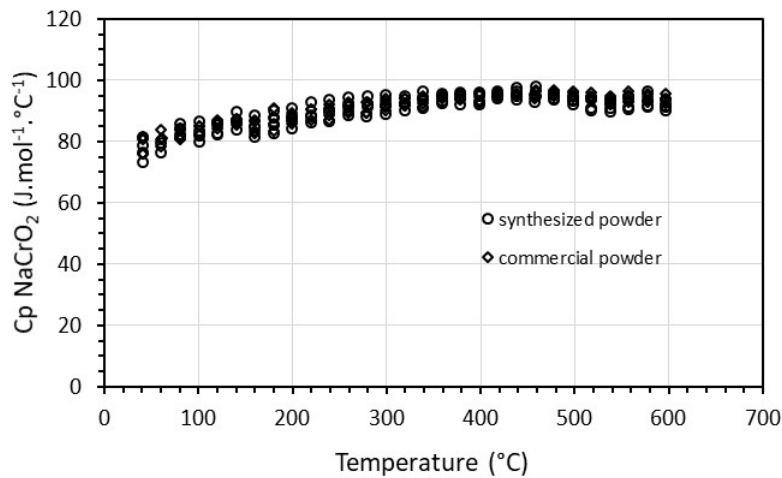


Figure 6. Cp evolution for the experimental and commercial NaCrO₂ powders versus temperature

Our experimental results were fitted with a polynomial law contrary to Sreedharan *et al.* [6] and Iyer *et al.* [16] who fitted their data with a linear law. We found:

$$C_p (J.K^{-1}.mol^{-1}) = -80.575 + 0.04736 \times T(K) - 2.9 \times 10^{-5} \times T(K)^2 - 1641963 / T(K)^2 (\pm 1.5 \%)$$

If we compare our experimental results with the experimental values of Sreedharan *et al.* [6] obtained also by DSC and of Iyer *et al.* [16] deduced from enthalpic increment using a Calvet microcalorimeter and with the data calculated with the quasi-harmonic model (see part 5.), we note that we are in good agreement with Iyer *et al.* (Figure 7). The heat capacities deduced from the quasi-harmonic model are slightly higher than the experimental ones. This behavior can not be explained according to the parameters of the quasi-harmonic model V_0 , B_0 , B'_0 , vibration frequencies and the Vinet EOS. Only the ab initio calculations of $E(V)$ and the vibration frequencies, starting point of the whole study, are to be called into question.

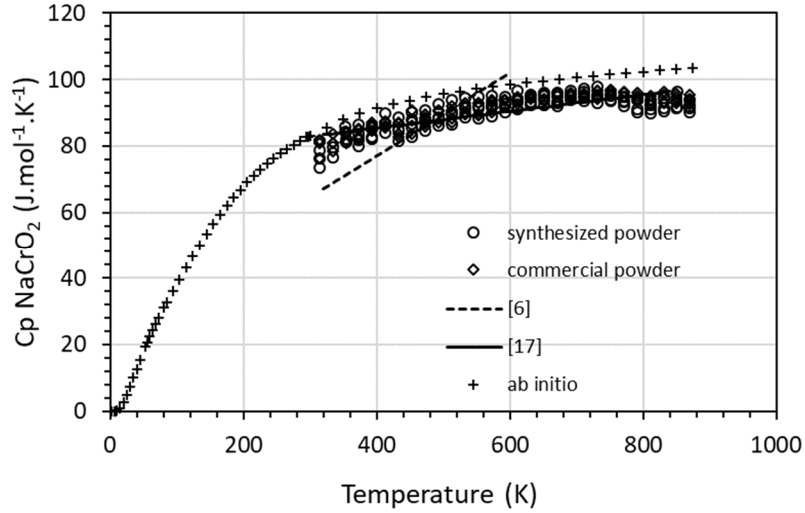


Figure 7. Comparison of the Cp measurements with literature and calculated data

The Gibbs energy of formation of NaCrO_2 with temperature can be deduced from Cp measurements using for the entropy and the enthalpy of formation at 298 K respectively $S^\circ_{298\text{K}}=94.53 \text{ J. mol}^{-1}. \text{ K}^{-1}$ (deduced from *ab initio* calculations, see 5.2) and $\Delta_f H^\circ_{298\text{K}}=-874.2\pm 7.3 \text{ kJ.mol}^{-1}$ [13] (equations 6 to 8). The data for pure elements are from JANAF tables [14].

$$\Delta_f G^\circ(T) = \Delta_f H^\circ(T) - T\Delta S^\circ(T) \quad (6)$$

$$\Delta_f H^\circ(T) = \Delta_f H^\circ_{298 \text{ K}} + \int_{298.15}^T C_p(T) dT - \sum [H^\circ(T) - H^\circ_{298 \text{ K}}]_{\text{elements}} \quad (7)$$

$$\Delta S^\circ(T) = S^\circ_{298 \text{ K}} + \int_{298.15}^T [C_p^\circ(T)/T] dT - \sum S^\circ(T)_{\text{elements}} \quad (8)$$

We obtained:

$$\Delta_f G^\circ(T) (\text{NaCrO}_2) (\text{kJ/mol O}_2) = -876.094 + 0.191 \times T (\pm 2\%).$$

The data are plotted Figure 8 and compared with the weighted regression proposed by Pillai *et al.* [2] after analysis of the reliable measurements reported in the literature and the values calculated using the heat capacity results of Iyer *et al.* [17] and Sreedharan *et al.* [6]. Gibbs energy of formation calculated combining our heat capacity results (experimental and theoretical) with enthalpy of formation published by Jain *et al.* [16] and Gross *et al.* [13] are also included.

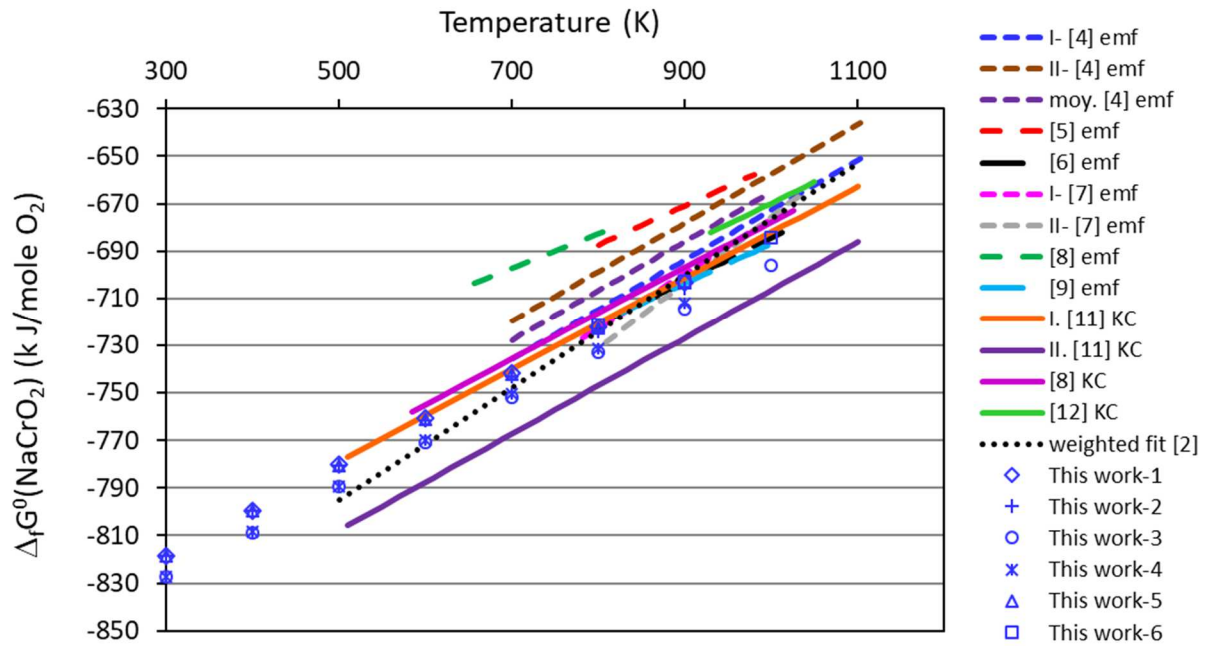


Figure 8. Gibbs energy of formation of NaCrO_2 deduced from this work compared to the experimental data of the literature and the weighted regression of [2]. Gibbs energy of formation calculated using our experimental C_p and $\Delta_f H^\circ_{298\text{ K}}$ value from [13] (This work- 1), our theoretical C_p and $\Delta_f H^\circ_{298\text{ K}}$ value from [13] (This work- 2), our theoretical the C_p and $\Delta_f H^\circ_{298\text{ K}}$ value from [16] (This work- 3), our experimental C_p and $\Delta_f H^\circ_{298\text{ K}}$ value from [16] (this work- 4), experimental C_p [17] and $\Delta_f H^\circ_{298\text{ K}}$ value from [13] (This work- 5) and experimental C_p [6] and $\Delta_f H^\circ_{298\text{ K}}$ value from [13] (This work- 6).

We note that the heat of formation at 298 K is the preponderant value for the Gibbs energy of formation calculation compared to the heat capacity as we obtain the almost identical results whatever the heat capacity values (the difference is maximum 2 kJ/mol). Our results are in good agreement with one of the results of Knights deduced from mass spectrometry measurements over $\text{NaCrO}_2(\text{s})\text{-Cr}_2\text{O}_3(\text{s})\text{-Cr}(\text{s})$ equilibrium [11] in the all temperature range and with [6] and [9] data. The discrepancy is much larger with equilibria involving liquid sodium [5] [8].

6.2- Decomposition temperature of NaCrO_2

We obtained a temperature of 819 ± 4 $^\circ\text{C}$ slightly higher than the value of Barker *et al.* of 795 $^\circ\text{C}$. However, X-ray analysis of the samples indicated only the NaCrO_2 phase (Figure 9). A heat treatment at 825 $^\circ\text{C}$ during 5 hours in a sealed quartz ampoule was then carried out for the two kinds of NaCrO_2 . In this case also, only NaCrO_2 was found by XRD. We can thus not confirm that this temperature is the decomposition temperature.

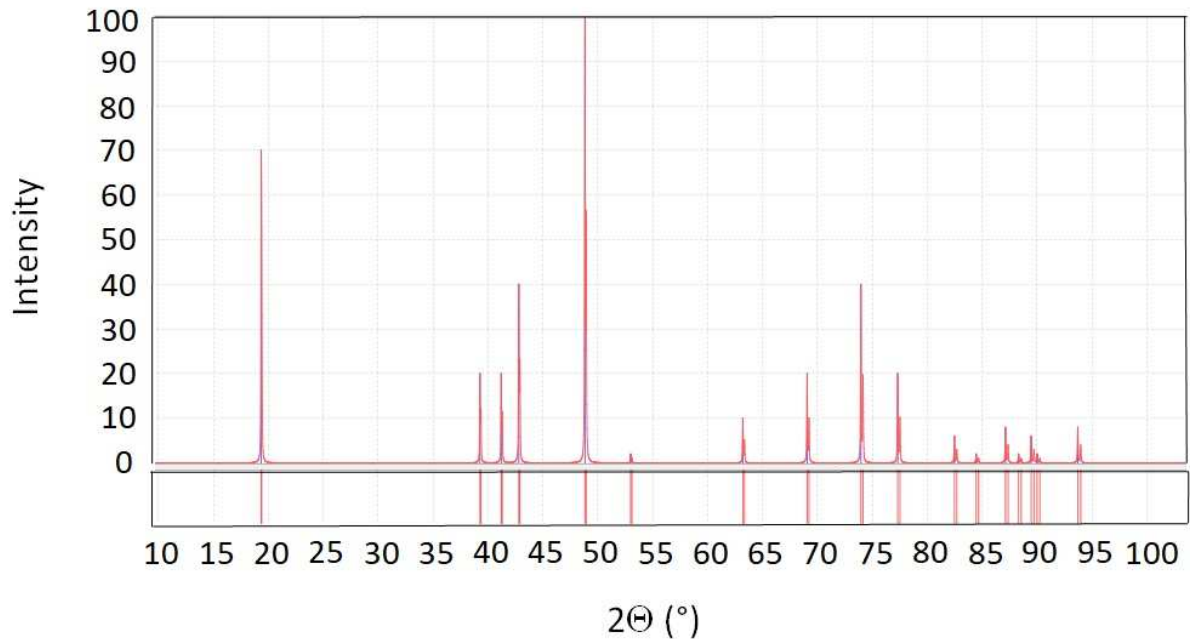


Figure 9. Indexation of X-ray diffractogram of NaCrO_2 powder after a heat treatment at 825°C during 5 hours with NaCrO_2 angles.

7- Conclusion

The sodium chromite NaCrO_2 is the main corrosion product of stainless steel corrosion in liquid sodium. Accurate Gibbs energy of formation is necessary to compute the threshold oxygen levels in liquid sodium for NaCrO_2 formation. A lot of studies have been performed but results are scattered. So to improve the accuracy of thermodynamic properties of NaCrO_2 heat capacity measurements were undertaken by DSC on commercial and synthesized NaCrO_2 powder between 25°C and 600°C and calculated using DFT. Gibbs energy of formation versus temperature was deduced combining enthalpy of formation value at 25°C from Gross *et al.* [13] and the entropy deduced from *ab initio* calculations performed in this work at 25°C . These results are in good agreement with other experimental data [6] [9] [11] which stabilize the compound. The Gibbs energy of formation calculated is more sensitive to the enthalpy of formation at 298 K than to the heat capacity or entropy ones. The stability of the sodium chromite was studied by DTA. We found a temperature of phase transformation at $819\pm 4^\circ\text{C}$ which is slightly higher than the decomposition temperature of 795°C proposed by Barker *et al.* However, the XRD analysis identified showed only the NaCrO_2 phase which does not confirm the NaCrO decomposition. Further investigations must be undertaken to identify the nature of this transition.

Acknowledgements

The authors gratefully acknowledge A. Lequien and R. Guillou (CEA-DMN-SRMA) for the X ray diffraction analysis and M. Tabarant (CEA-DPC-SEARS) for the Glow Discharge Mass Spectrometry measurements.

References

[1] C.K. Mathew, Thermochemistry of fuel-clad and clad-coolant interactions of fast breeder reactors, *Pure&Appl. Chem.* 67 (1995) 1011-1018. <https://doi.org/10.1351/pac199567061011>

- [2] S.R. Pillai, H.S. Khatak, J.B. Gnanamoorthy, Formation of NaCrO_2 in sodium systems for fast reactors and its consequence on the carbon potential, *J. Nucl. Mater.*; 224 (1995) 17-24.
[https://doi.org/10.1016/0022-3115\(95\)00038-0](https://doi.org/10.1016/0022-3115(95)00038-0)
- [3] S.A. Jansson and E. Berkey, Oxidation-reduction reactions for chromium and 304 stainless steel in liquid sodium, *Corrosion by liquid metals*, Eds J.E. Draley and J.R. Weeks (Plenum Press, New-York) (1970) p. 479-513
- [4] B.J. Shaiu, P.C.S Wu and P. Chiotti, Thermodynamic properties of the double oxides of Na_2O with the oxides of Cr, Ni and Fe, *J. Nucl. Mater.* 67 (1977) 13-23. [https://doi.org/10.1016/0022-3115\(77\)90157-X](https://doi.org/10.1016/0022-3115(77)90157-X)
- [5] S.A. Frankham, *Materials Behaviour in the Liquid Alkali Metals Lithium and Sodium*, Ph. D Thesis, University of Nottingham UK (1982) p. 209-222
- [6] O.M. Sreedharan, B.S. Madan and J.B. Gnanamoorthy, Threshold oxygen levels in Na(l) for the formation of $\text{NaCrO}_2(\text{s})$ on 18-8 stainless steels from accurate thermodynamic measurements, *J. Nucl. Mater.* 119 (1983) 296-300. [https://doi.org/10.1016/0022-3115\(83\)90207-6](https://doi.org/10.1016/0022-3115(83)90207-6)
- [7] N.P. Bhat, K. Swaminathan, D. Krishnamurthy, O.M. Sreedharan, M. Sundaresan, Thermochemical studies on lithium chromite, *Proc. 3rd Int. Conf. on Liquid Metal Engineering and Technology*, Oxford, The British Nuclear Energy Society, London, (1984) Vol. I, p.323-327
- [8] T. Gnanasekaran and C.K. Mathews, Threshold oxygen levels in sodium necessary for the formation of NaCrO_2 in sodium-steel systems, *J. Nucl. Mater.* 140 (1986) 202-213.
[https://doi.org/10.1016/0022-3115\(86\)90203-5](https://doi.org/10.1016/0022-3115(86)90203-5)
- [9] V. Venugopal, V.S. Iyer, V. Sundaresan, Z. Singh, R. Prasad and D.D. Sood, Standard molar Gibbs energy of formation of NaCrO_2 by e.m.f measurements, *J. Chem. Thermodynamics* 19 (1987) 19-25.
[https://doi.org/10.1016/0021-9614\(87\)90157-1](https://doi.org/10.1016/0021-9614(87)90157-1)
- [10] Blokhin, V.A., Borisov, V.V., Kamaev, A.A., Levin, O.E, Stroyev, V.A., Trufanov, A.A, *Problems of atomic science and technology. Series: Nuclear and reactor constants, Thermodynamic potential electrode Na-Cr- NaCrO_2* , 3 (2017) p. 171-176
- [11] C.F. Knights and B.A. Philipps, Phase diagrams and thermodynamic studies of the Cs-Cr-O, Na-Cr-O and Na-Fe-O systems and their relationships to the corrosion of steels by caesium and sodium, *Proc. High temperature chemistry of inorganic and ceramic materials*, Ed. F.P. Glassner and P.E. Potter (1976), p. 134-145
- [12] S. Dash, Z. Singh, R. Prasad and D.D. Sood, Standard molar Gibbs free energies of formation of LiCrO_2 and of NaCrO_2 , *J. Chem. Thermodynamics* 22 (1990) 61-66. [https://doi.org/10.1016/0021-9614\(90\)90031-K](https://doi.org/10.1016/0021-9614(90)90031-K)
- [13] P. Gross, G.L. Wilson and W.A. Gutteridge, Composition and Heat of Combination of a Double Oxide of Chromium and Sodium, *J. Chem. Soc. (A)* 1970 1908-1913.
<https://doi.org/10.1039/J19700001908>
- [14] *J. Physical and Chemical Reference Data, Monograph N° 9, NIST-JANAF Thermochemical Tables, Fourth Edition*, M.W. Chase, Jr., American Chemical Society and American Institute for Physics, 1998
- [15] C.P.J. Van Vuuren, A thermoanalytical study of the synthesis and oxidation of NaCrO_2 , *Thermochimica Acta* 168 (1990) 135-141. [https://doi.org/10.1016/0040-6031\(90\)80633-A](https://doi.org/10.1016/0040-6031(90)80633-A)
- [16] A. Jain, G. Hautier, S.P. Ong, C.J. Moore, C.C. Fischer, K.A. Persson, and G. Ceder, Formation enthalpies by mixing GGA and GGA+U calculations, *Phys. Rev. B* 84 (2011) 045115.
<https://doi.org/10.1103/PhysRevB.84.045115>

- [17] V.S. Iyer, K. Jayanthi, G.A. Ramarao, V. Venugopal, D.D. Sood, Enthalpy increment measurements of NaCrO₂ using a high temperature Calvet calorimeter, *J. Nucl. Mater.* 183 (1991) 76-79. [https://doi.org/10.1016/0022-3115\(91\)90473-K](https://doi.org/10.1016/0022-3115(91)90473-K)
- [18] M.G. Barker and A.J. Hooper, Reactions of chromium oxides and chromium metal with disodium oxide, *J. Chem. Soc. Dalton* (1975) 2487-2489. <https://doi.org/10.1039/DT9750002487>
- [19] S. Sampath, S.K. Sali and N.C. Jayadevan, Thermochemical studies in the sodium-chromium-oxygen system, *Thermochimica Acta* 159 (1990) 327-335. [https://doi.org/10.1016/0040-6031\(90\)80118-I](https://doi.org/10.1016/0040-6031(90)80118-I)
- [20] S. Komaba, C. Takei, T. Nakayama, A. Ogata, N. Yabuuchi, Electrochemical intercalation activity of layered NaCrO₂ vs. LiCrO₂. *Electrochemistry Communications* 12 (2010) 355–358. <https://doi.org/10.1016/j.elecom.2009.12.033>
- [21] A. Fukunaga, T. Nohira, Y. Kozawa, R. Hagiwara, S. Sakai, K. Nitta, S. Inazawa, Intermediate-temperature ionic liquid NaFSA-KFSA and its application to sodium secondary batteries, *Journal of Power Sources* 209 (2012) 52–56. <https://doi.org/10.1016/j.jpowsour.2012.02.058>
- [22] J.J. Ding, Y.N. Zhou, Q. Sun, Z.W. Fu, Cycle performance improvement of NaCrO₂ cathode by carbon coating for sodium ion batteries, *Electrochemistry Communications* 22 (2012) 85–88. <https://doi.org/10.1016/j.elecom.2012.06.001>
- [23] W. Scheld and R. Hoppe, On the α -NaFeO₂ type - About NaCrO₂ and KCrO₂, *Z. anorg. Allg. Chem.* 568 (1989) 151-156
- [24] C.Y. Chen, K. Matsumoto, T. Nohira, R. Hagiwara, A. Fukunaga, S. Sakai, K. Nitta, S. Inazawa, Electrochemical and structural investigation of NaCrO₂ as a positive electrode for sodium secondary battery using inorganic ionic liquid NaFSA–KFSA, *Journal of Power Sources* 237 (2013) 52–57. <https://doi.org/10.1016/j.jpowsour.2013.03.006>
- [25] J. L. Fleche, Thermodynamical functions for crystals with large unit cells such as zircon, coffinite, fluorapatite, and iodoapatite from *ab initio* calculations, *Physical Review B* 65 (2002) 245116.1-245116.10. <https://doi.org/10.1103/PhysRevB.65.245116>
- [26] S. J. Clark, M. D. Segall, C. J. Pickard, P. J. Hasnip, M. J. Probert, K. Refson, and M. C. Payne, First principles methods using CASTEP, *Zeitschrift für Kristallographie* 220(5-6) (2005) 567-570. <https://doi.org/10.1524/zkri.220.5.567.65075>
- [27] D. Vanderbilt, Soft self-consistent pseudopotentials in a generalized eigenvalue formalism, *Phys. Rev. B* 41 (1990) 7892-7895. <https://doi.org/10.1103/PhysRevB.41>.
- [28] J. P. Perdew, K. Burke, and M. Ernzerhof, Generalized gradient approximation made simple, *Phys. Rev. Lett.* 77 (1996) 3865-3868. <https://doi.org/10.1103/PhysRevLett.77.3865>
- [29] J. D. Pack and H. J. Monkhorst, Special points for Brillouin-zone integration – a reply, *Phys. Rev. B* 16 (1977) 1748. <https://doi.org/10.1103/PhysRevB.16.1748>
- [30] P. Vinet, J. R. Smith, J. Ferrante, and J. H. Rose, Temperature effects on the universal equation of state of solid, *Phys. Rev. B* 35 (1987) 1945-1953. <https://doi.org/10.1103/PhysRevB.35.1945>.